

Electrochemical properties of intermediate-temperature SOFCs based on proton conducting Sm-doped BaCeO₃ electrolyte thin film

Peng Ranran^a, Wu Yan^b, Yang Lizhai^a, Mao Zongqiang^{a,*}

^a Institute of Nuclear and New Energy Technology, Tsinghua University, Beijing, 100084, P.R. China

^b Faculty of Material Science and Chemical Engineering, China University of Geosciences, Wuhan 430074, P.R. China

Received 31 August 2005; received in revised form 18 November 2005; accepted 26 November 2005

Abstract

Dense BaCe_{0.8}Sm_{0.2}O_{2.90} (BCSO) thin films were successfully fabricated on porous NiO–BCSO substrates by dry pressing process. As characterized by scanning electron microscope, the BCSO films were about 50 μm. With Ba_{0.5}Sr_{0.5}Co_{0.8}Fe_{0.2}O_{3–δ} (BSCF) as cathodes, single cells were tested at 600 and 700 °C with humidified (3% HB₂O) hydrogen as fuel and oxygen as oxidant. The open circuit voltage of 1.049 V at 600 °C and 1.032 V at 700 °C were achieved, indicating negligible gas permeation through the BCSO thin films. Maximum power densities of 132 and 340 mW/cm² were obtained at 600 and 700 °C, respectively. The impedance measurements at open circuit conditions showed that there were two rate-limiting processes for the electrode reactions and that the cell performances were essentially determined by the electrode polarization resistances at temperature below 650 °C, which implied that it was essential to reduce the electrode polarization by developing novel electrode materials to improve the performance of ITSOFC based on BCSO electrolyte. Conductivities of BCSO under the cell operating circumstances were obtained as 0.00416, 0.00662 and 0.00938 Scm⁻¹ at 500, 600 and 700 °C, respectively. The activation energy of BCSO conductivity was calculated as 29.5 and 43.8 kJ/mol for the temperature range of 550–700 °C and of 400–550 °C, respectively. Endurance test was firstly carried out with 75 μm BCSO electrolyte at 650 °C at the operating voltage of 0.7 V and current density about 0.12 A/cm². Both voltage and current density remained stable for 1000 min.

© 2005 Elsevier B.V. All rights reserved.

PACS: 82.47.Ed

Keywords: Solid oxide fuel cell; High temperature protonic ceramics; Doped barium cerate; Thin film fabrication; AC impedance

1. Introduction

Solid oxide fuel cells (SOFC) have gained many attentions due to their high thermodynamic efficiency and low impact to the environment, as a promising energy conversion system. But the high operating temperature (up to 1000 °C) of classical SOFCs with stabilized zirconia as electrolyte can lead to complex materials problems such as electrode sintering, interfacial diffusion, and especially the preparation of hermetic seals and interconnect. Great efforts have been devoted to developing solid oxide fuel cells (SOFCs) capable of operating at intermediate temperature by adopting novel electrolyte with high ionic conductivity (such as doped ceria) and developing thin film fabrication technology. And considerable achievements have been gained [1–5].

Although current SOFC technology based on oxide ion conductors, such as stabilized zirconia and doped ceria, is well established, there are still many problems with respect to the materials incompatibility and the poor intrinsic fuel utilization due to the water vapor produced at the anode. It's deemed that developing novel electrolyte materials for SOFC is crucial for the commercial development of SOFC.

Doped barium cerate (BaCeO₃) materials have drawn special attention as the substitute electrolyte materials for LTSOFC for their high proton conduction over the wide temperature range of 300 to 1000 °C. Although the conductivities of presently available BaCeO₃ are no higher than those of the doped ceria, these materials have the possibility to meet the criterion as LTSOFC electrolyte for the following four reasons. First, the proton conduction of BaCeO₃ leads to the water vapor produced at the cathode side, which helps to improve the EMF and the conversion efficiency of SOFC system [6]. Second, proton conduction in BaCeO₃ is governed

* Corresponding author. Tel.: +86 10 62784827.

E-mail address: maozq@tsinghua.edu.cn (M. Zongqiang).

by a mechanism based on the hopping of an extremely small proton between adjacent oxide ions, which could result in lower activation energies than those for oxide-ion conduction in YSZ and the doped ceria [7]. Third, the electronic conductivity of BaCeO_3 is much lower than that of doped ceria under the operating circumstance, and thus, the cell EMF, power output and conversion efficiency could be intensively improved [8]. Fourth, the solubility of protons in the BaCeO_3 bulk increases with the decrease of temperature which could enhance the preexponential of proton conduction with the decreasing temperature [9,10]. All these imply that doped BaCeO_3 should be more appropriate for the application of SOFCs electrolytes at reduced operating temperature.

High efficiency and high conductivity promote the application of doped barium cerate materials to SOFC electrolyte. Yet, due to the low sinterability of BaCeO_3 and insufficient technology develop, electrolyte-supported configuration was always adopted with the thickness of BaCeO_3 about 0.5 mm, and therefore, the maximum power densities of such SOFCs are only about tens of mW/cm^2 at 700 °C [11–16], much lower than conventional oxygen ion conducting SOFC. To improve the performance of SOFC based on BaCeO_3 electrolyte, configuration optimization must be made. In this study, we focused on the fabrication of dense Sm-doped BaCeO_3 thin film on the porous anode substrate. Electrochemical characteristics of a single SOFC with BCSO electrolyte were thus studied.

2. Experimental

$\text{BaCe}_{0.8}\text{Sm}_{0.2}\text{O}_{2.9}$ (BCSO) powders were synthesized by modified glycine-nitrate process (GNP). $\text{Ba}(\text{C}_2\text{H}_3\text{O}_2)_2$, $\text{Ce}(\text{NO}_3)_3 \cdot 6\text{H}_2\text{O}$ and $\text{Sm}(\text{NO}_3)_3$ were dissolved at the stoichiometric ratio and glycine was then added with the glycine/metal mole ratio set at 1. The solution was heated under stirring, converted to a viscous gel and ignited to flame, resulting in the pale yellow ash. The ash was calcined at 1100 °C for 4 h to remove any carbon residues and to form the stable oxide of BCSO.

NiO and BSCO powders were blended and pressed under 200 MPa as a green substrate with 13 mm in diameter and 0.65 mm in thickness. The BSCO powders and the substrate were then co-pressed at 250 MPa to form a green bilayer and subsequently co-fired at 1350 °C in air for 5 h to densify the BSCO film. The thickness of the electrolyte was controlled at 50 or 75 μm by adopting appropriate amount of BCSO powders. Slurry consisting of $\text{Ba}_{0.5}\text{Sr}_{0.5}\text{Co}_{0.8}\text{Fe}_{0.2}\text{O}_{3-\delta}$ (BCSF) and BSCO was applied to the electrolyte by printing and then fired at 1100 °C in air for 4 h to form a porous cathode. Ag paste was applied on the electrodes as current collector followed by calcination at 873 K for 30 min.

The phase identification of the sintered anode-electrolyte bilayer was studied with the powder X-ray diffraction by Cu-K_α radiation (Bruker cop. Germany).

Single cells were tested at 600 and 700 °C in a home-developed-cell-testing system with humidified hydrogen ($\sim 3\%$ H_2O) as fuel and oxygen as oxidant, respectively. Fuel-cell performances were measured with an EG&G potentiostat/galvanostat (Model 273A) interfaced with a computer. A

scanning electron microscope (SEM, JSM-6301F) was used to detect the microstructure of the tested cells.

Resistances of the cells under open circuit conditions were investigated by AC impedance spectroscopy at the temperature from 400 to 700 °C using a PerkinElmer 5210 frequency response analyzer (0.5 Hz to 120 KHz) combined with EG&G PAR potentiostat/galvanostat 263 A.

3. Results and discussion

Dry-pressing is a simple, reproducible, and cost-effective method for thin film fabrication, in which the thickness of the thin film could be easily controlled by adopting suitable amount of the powders. Calculating from the theoretical density of $\text{BaCe}_{0.8}\text{Sm}_{0.2}\text{O}_{2.9}$ (BCSO) combined with the radial sintering shrinkage of anode/electrolyte bilayer, we prepared the electrolyte films of 50 and 75 μm on the porous anodes.

Fig. 1 presents the XRD spectra of anode/electrolyte bilayer sintered at 1350 °C for 5 h. It could be clearly seen that there were only peaks corresponding to $\text{BaCe}_{0.8}\text{Sm}_{0.2}\text{O}_{2.9}$ in electrolyte film and to NiO and $\text{BaCe}_{0.8}\text{Sm}_{0.2}\text{O}_{2.9}$ in the anode substrate, which gave no evidence for the formation of other substance.

The cross-section view of a post-test cell with the structure of Ni–BCSO/BCSO/BCSF–BCSO was shown in Fig. 2. In this case, the BCSO film was about 50 μm thick, quite dense, uniform and adhered very well to Ni–BCSO anode substrate and BCSF–BCSO cathode (about 35 μm thick). Fig. 3 gave the electrical performance of the single cell as a function of current density and operating temperature. The open circuit voltage (OCV) was over 1.0 V in humid H_2 and O_2 system, which was close to the theoretical value and indicated that the BCSO film fabricated on the porous Ni–BCSO substrate has enough density to prevent gas leakage through it. An open circuit voltage (OCV) of about 1.049 V was achieved at 600 °C, and 1.032 V at 700 °C, respectively. Maximum power densities were obtained about 132 mW/cm^2 at 600 °C, and 340 mW/cm^2 at 700 °C, respectively. This result was much higher than the

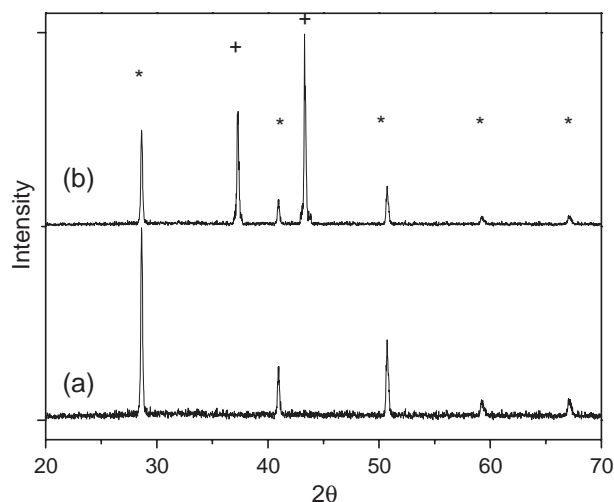


Fig. 1. XRD spectra for the bilayer of BCSO film (a) and NiO–BCSO anode substrate (b) sintered at 1350 °C. *: BCSO; +: NiO.

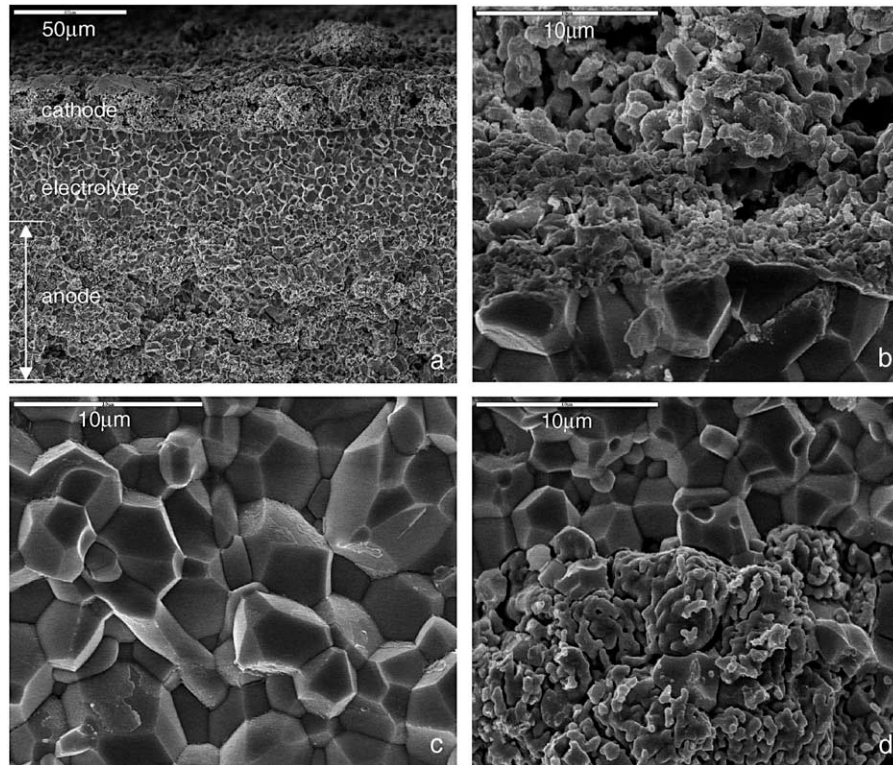


Fig. 2. Cross-section images of the tested cell with BCSF–BCSO, BCSO and Ni–BCSO as cathode, electrolyte and anode from top to bottom. a) single cell (b) cathode/electrolyte (c) electrolyte (d) electrolyte/anode.

forgoing results based on the protonic SOFC, but still not satisfactory compared to the cell based on samaria-doped ceria (SDC) films about 20 μm thick, for which maximum power densities were 397 mW/cm^2 at 600 $^\circ\text{C}$ [17]. It's deemed that intensively reducing the thickness of BCSO film to about 20 μm should improve the output of the cell. Bulk resistances of the cell were obtained as 1.976 and 0.818 $\Omega \text{ cm}^{-2}$ at 600 and 700 $^\circ\text{C}$, respectively, by fitting the linear region of I – V curves as denoted by the dash line in Fig. 3.

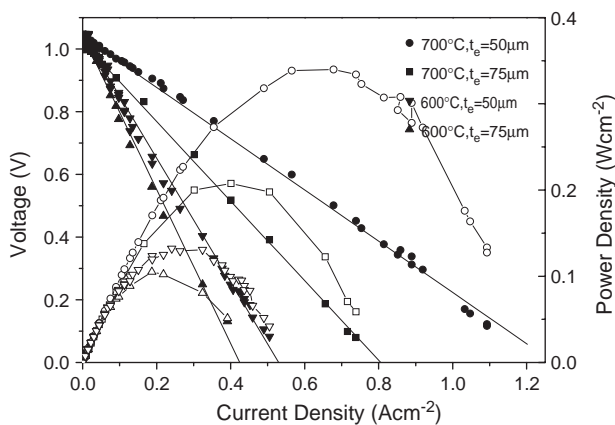


Fig. 3. Cell voltage (solid) and power density (hollow) as a function of current density for the cell consisted of NiO– $\text{BaCe}_{0.8}\text{Sm}_{0.2}\text{O}_{2.9\text{B}}$ as composite anode, $\text{BaCe}_{0.8}\text{Sm}_{0.2}\text{O}_{2.9}$ as electrolyte and $\text{Ba}_{0.5}\text{Sr}_{0.5}\text{Co}_{0.8}\text{BFe}_{0.2}\text{OB}_{3-\delta}$ – $\text{BaCe}_{0.8}\text{Sm}_{0.2}\text{O}_{2.9}$ as composite cathode. t_e gives the thickness of the cell electrolyte.

Fig. 3 also gave the electrical performance of the single cell with the BCSO film of 75 μm in thickness of which OCV was 1.043 V at 600 $^\circ\text{C}$ and 1.029 V at 700 $^\circ\text{C}$, respectively. Maximum power densities were obtained about 105 and 208 mW/cm^2 at 600 and 700 $^\circ\text{C}$, respectively. Bulk resistances of the cell were figured by fitting the linear region of I – V curves as 2.459 and 1.270 $\Omega \text{ cm}^{-2}$ at 600 and 700 $^\circ\text{C}$, respectively.

To intensively explore the electrical characteristics of the cell, AC impedance characteristics of the cell with 75 μm BCSO film was measured at the open circuit condition from 450 to 700 $^\circ\text{C}$. Fig. 4 presented the effect of operating temperature on the impedance characteristics. It could be clearly seen that each impedance spectra corresponded to two overlapping arcs (depressed semicircles), which were taken as the polarization resistance of the electrodes and implied that there were two rate-limiting processes for the electrode reaction. The arc corresponding to lower frequencies was dominant and increased dramatically with the decrease of operating temperature, while the arc corresponding to higher frequency increased relatively slower than the former. Fig. 4(a) illustrated the composition of the cell resistance, where R_b was the electrolyte resistance, R_p was the electrode polarization resistance and R_{total} was the total cell resistance.

Shown in Fig. 5 was the total cell resistance, the interfacial resistance and electrolyte resistance as determined from the impedance spectra. Both the electrolyte resistance and polarization resistances decreased with the increase of temperature and the interfacial resistances exceeded the resistances of the

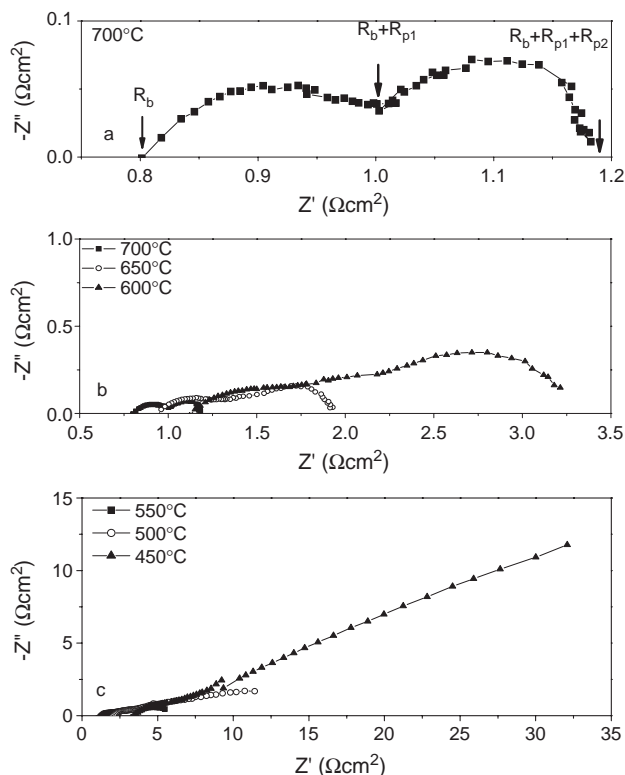


Fig. 4. Impedance spectra of a single cell with a 50 μm thick BCSO film measured at different temperature. (a) 700, (b) 600–700, and (c) 450–550 °C.

electrolyte at temperature below 650 °C. The ratio of the electrolyte resistance to the cell resistance decreased markedly as the operating temperature was reduced, about 0.689 at 700 °C to 0.155 at 500 °C, as shown in Fig. 5. This implies that developing novel electrode materials is essential to improve the performance of the BCSO-based fuel cells. Hibino et al. adopted 3 wt.% Pd-loaded FeO and $Ba_{0.5}Pr_{0.5}CoO_3$ as the anode and the cathode, and a peak power density of 134 mW cm² was attained at 600 °C using an even 0.5 mm thick $BaCe_{0.75}Y_{0.25}O_{3-\delta}$ electrolyte, which gave light to the novel electrode developing [18].

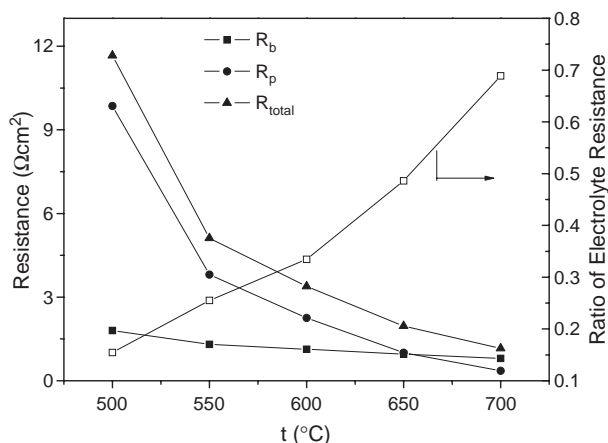


Fig. 5. The total cell resistances (R_{total}), interfacial polarization resistances (R_p), electrolyte resistances (R_b) and the ratio of electrolyte resistance to total resistance (□) obtained from impedance spectra at different temperatures.

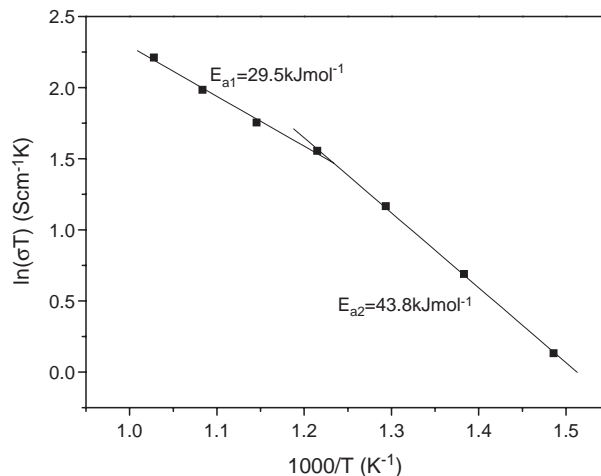


Fig. 6. Arrhenius plots of $BaCe_{0.8}Sm_{0.2}O_{2.9}$ conductivities under the cell operating circumstance determined by impedance spectra. E_a is the active energy of conductivity.

Fig. 6 presented the Arrhenius plots of BCSO electrolyte calculated from the cell impedance characteristics. It's noted that the curve had two regimes with different slope intersecting at about 550 °C. As a mixed conductor, BCSO electrolytes show not only proton but also oxide-ion conduction under the fuel cell operating circumstance. The protonic conductivity was reported to preponderate over oxide-ion conductivity at temperature lower than 800 °C and to be about one order higher than it at temperature lower than 600 °C. The dominance of protonic conductivity at operating temperature might suggest that the intersection of conductivity comes not from the change of conducting species but from the dependence of protonic defects concentration on temperature, which is quite accordant with literature [10]. The activation energy was calculated as 29.5 and 43.8 kJ/mol for the temperature range of 550–700 and of 400–550 °C, respectively. Conductivities of BCSO under the operating circumstances were obtained as 0.00416, 0.00662 and 0.00938 Scm⁻¹ at 500, 600 and 700 °C, respectively.

Chemical stability in the working environment is a major factor for electrolyte materials. And it might be a severe

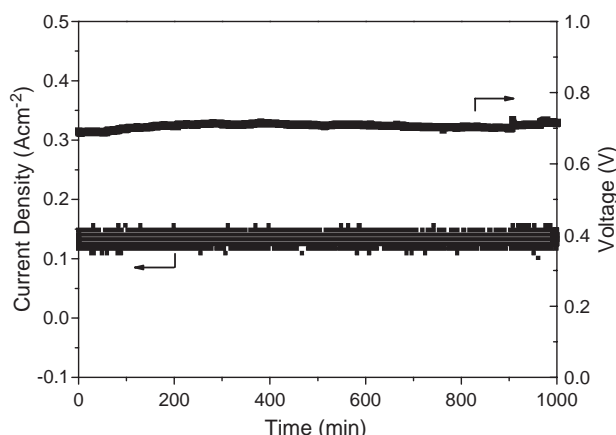


Fig. 7. Short-term stability of the cell with 75 μm thick BCSO tested at 650 °C at the voltage of 0.7 V with humid H₂ and O₂.

problem for BCSO for the possibility of forming alkaline earth hydroxides at high water activities. Endurance test of the present fuel cell with 75 μm BCSO electrolyte was carried out at 650 $^{\circ}\text{C}$ at the operating voltage of 0.7 V and current density about 0.12 A/cm^2 . As shown in Fig. 7, there was no obvious decline for both voltage and current density for 1000 min, implying the stability of the BCSO electrolyte and the strong junction between the electrolyte and the electrode.

4. Conclusions

$\text{BaCe}_{0.8}\text{Sm}_{0.2}\text{O}_{2.90}$ (BCSO) thin films of 50 μm in thickness were successfully fabricated on porous NiO–BCSO substrate by dry pressing process. The sintered BCSO film was quite dense, uniform and adhered well to both electrodes. The open circuit voltage of 1.049 V at 600 $^{\circ}\text{C}$ and 1.032 V at 700 $^{\circ}\text{C}$ was achieved, respectively, when the BCSO-based cells were tested with humidified hydrogen as fuel and air as oxidant. Maximum power densities of 132 and 340 mW/cm^2 were obtained at 600 and 700 $^{\circ}\text{C}$, respectively. The impedance measurements at open cell conditions showed that there were two rate-limiting processes for the electrode reactions and that the cell performances were essentially determined by the electrode polarization resistances at temperature below 650 $^{\circ}\text{C}$. Conductivities of BCSO under the cell operating circumstances were obtained as 0.00416, 0.00662 and 0.00938 Scm^{-1} at 500, 600 and 700 $^{\circ}\text{C}$, respectively. The activation energy of BCSO conductivity was calculated as 29.5 and 43.8 kJ/mol for the temperature range of 550–700 $^{\circ}\text{C}$ and of 400–550 $^{\circ}\text{C}$, respectively. Endurance test was carried out at 650 $^{\circ}\text{C}$ with 75 μm BCSO electrolyte at the operating voltage of 0.7 V and current density about 0.12 A/cm^2 . Both voltage and current density remained stable for 1000 min.

Acknowledgements

This work was supported by China National Hydrogen project (contract no. G2000026410 and 2001AA515080) and by the State Key Laboratory of Automotive Safety and Energy in Tsinghua University.

References

- [1] T. Ishihara, M. Honda, T. Shibayama, H. Minami, Y. Takita, *J. Electrochem. Soc.* 145 (1998) 3177.
- [2] Changrong Xia, Meilin Liu, *Solid State Ion.* 144 (2001) 249.
- [3] Zongping Shao, Sossina M. Haile, *Nature* 431 (2004) 170.
- [4] K. Kobayashi, I. Takahashi, M. Shiono, M. Dokiya, *Solid State Ion.* 152–153 (2002) 591.
- [5] Z. Cai, T.N. Lan, S. Wang, M. Dokiya, *Solid State Ion.* 152–153 (2002) 583.
- [6] Anatoly Demin, Panagiotis Tsiakaras, *Int. J. Hydrogen Energy* 26 (2001) 1103.
- [7] John B. Goodenough, *Annu. Rev. Mater. Res.* 33 (2003) 91.
- [8] Daisuke Hirabayashi, Atsuko Tomita, Shiny Teranishi, Takashi Hibino, Mitsuru Sano, *Solid State Ion.* 176 (2005) 881.
- [9] T. Hibino, K. Mizutani, T. Yajima, H. Iwahara, *Solid State Ion.* 57 (1992) 303.
- [10] K.D. Kreuer, *Annu. Rev. Mater. Res.* 33 (2003) 333.
- [11] H. Iwahara, *Solid State Ion.* 28–30 (1988) 573.
- [12] H. Iwahara, H. Uchida, K. Morimoto, *J. Electrochem. Soc.* 137 (1990) 462.
- [13] N. Bonanos, B. Ellis, M.N. Mahmood, *Solid State Ion.* 44 (1991) 305.
- [14] N. Tanigushi, K. Hatoh, J. Niikura, T. Gamo, *Solid State Ion.* 53–56 (1992) 998.
- [15] Iwahara Hiroyasu, Yajima Tamotsu, Ushida Harushisa, *J. Electrochem. Soc.* 140 (1993) 1687.
- [16] Bin Zhu, Xiangrong Liu, T. Schober, *Electrochem. Commun.* 6 (2004) 378.
- [17] C.R. Xia, F.L. Chen, M.L. Liu, *Electrochem. Solid-State Lett.* 4 (2001) A52.
- [18] Takashi Hibino, Atsuko Hashimoto, Masanori Suzuki, et al., *J. Electrochem. Soc.* 149 (2002) 1503.